

NACA RM L57D22b

~~CONFIDENTIAL~~Copy  
RM L57D22b

NACA

## RESEARCH MEMORANDUM

AERODYNAMICS OF OSCILLATING CONTROL SURFACES  
AT TRANSONIC SPEEDS

By Robert F. Thompson and Sherman A. Clevenson

Langley Aeronautical Laboratory  
Langley Field, Va.

LIBRARY COPY

JUN 20 1957

LANGLEY AERONAUTICAL LABORATORY  
LIBRARY, NACA  
LANGLEY FIELD, VIRGINIA

UNCLASSIFIED

By authority of NASA Class. Change Notices, Issue no. 3,

This material contains information affecting the National Defense of the United States within the meaning of the espionage laws, Title 18, U.S.C., Secs. 793 and 794, the transmission or revelation of which in any manner to an unauthorized person is prohibited by law.

dtd May 1, 1963; declassified Apr. 18, 1963. NLR-7-10-63.

NATIONAL ADVISORY COMMITTEE  
FOR AERONAUTICS

WASHINGTON

June 17, 1957

~~CONFIDENTIAL~~



3 1176 01437 9151

## NATIONAL ADVISORY COMMITTEE FOR AERONAUTICS

## RESEARCH MEMORANDUM

## AERODYNAMICS OF OSCILLATING CONTROL SURFACES

## AT TRANSONIC SPEEDS

By Robert F. Thompson and Sherman A. Clevenson

## SUMMARY

Oscillating flap-type and all-movable controls are discussed with particular emphasis on the aerodynamic forces and moments at transonic speeds. Hinge-moment results from recent wind-tunnel and rocket-powered-model tests are summarized for trailing-edge flap-type controls to illustrate the effects of control hinge-line position and profile shape on one-degree-of-freedom flutter of this type of control. From a wind-tunnel investigation of a model considered representative of an all-movable control, the aerodynamic effects due to rigid-body-oscillation modes in roll and in pitch are presented.

The general magnitudes of the unstable aerodynamic damping moments for the flap-type controls tested are presented. No significant benefits toward alleviating the unstable aerodynamic damping in the control rotational mode at transonic speeds were obtained for a wide range of hinge-line positions tested. Of three control profile modifications tested, only a "wedge" modification to a 35-percent-overhang balanced control gave significant improvements in "buzz" stability. This wedge control gave stable aerodynamic damping in the control rotational mode up to the maximum speed tested. However, the stable damping and improvement in flutter characteristics were limited to oscillation amplitudes less than about  $3^\circ$ .

For an all-movable control, the oscillating aerodynamic derivatives which define the separate effects of rigid-body pitch and rigid-body roll have been presented through the transonic speed range. The aerodynamic damping for this low-aspect-ratio all-movable control was stable at all conditions tested.

## INTRODUCTION

Oscillating aerodynamic forces and moments are needed in analyzing the dynamic or flutter characteristics of any airplane component. These aerodynamic values cannot be accurately computed for the mixed-flow

~~CONFIDENTIAL~~

conditions at transonic speeds, and there is a current need for experimental data. The purpose of this paper is to summarize some recent tests on oscillating flap-type and all-movable controls, wherein the aerodynamic effects at transonic speeds have been measured. Flap-type controls are discussed first, and results pertain primarily to one-degree-of-freedom flutter or "buzz." Then, the aerodynamic effects due to rigid-body modes in pitch and in roll are presented for an all-movable control.

## SYMBOLS

$c_a$	flap-type-control chord, distance from hinge line to trailing edge of control (see fig. 2), ft
$c_b$	flap-type-control balance chord, distance from hinge line forward to leading edge of control (see fig. 2), ft
$c_r$	root chord of all-movable control, ft
$c_t$	total control chord at midspan of control, $c_b + c_a$ , ft
$k_\alpha$	reduced frequency of all-movable-control pitch oscillation, $\frac{\omega c_r}{2V}$
$k_\delta$	reduced frequency of flap-type-control oscillation, $\frac{\omega c_t}{2V}$
$k_\phi$	reduced frequency of all-movable-control roll oscillation, $\frac{\omega c_r}{2V}$
$M$	free-stream Mach number
$M'$	area moment of flap-type-control area rearward of and about the hinge line, cu ft
$q$	free-stream dynamic pressure, lb/sq ft
$S$	semispan area of all-movable control, sq ft
$V$	free-stream velocity, ft/sec

$C_h$	flap-type-control hinge-moment coefficient, $\frac{\text{Hinge moment}}{2M'q}$
$C_L$	lift coefficient, $\frac{\text{Model lift}}{qS}$
$C_l$	rolling-moment coefficient (fig. 7), $\frac{\text{Model rolling moment about roll axis}}{qS \frac{C_r}{2}}$
$C_m$	pitching-moment coefficient (fig. 7), $\frac{\text{Model pitching moment about pitch axis}}{qS \frac{C_r}{2}}$
$\alpha$	amplitude of all-movable-control pitch oscillation, radians except as noted
$\delta$	amplitude of flap-type-control oscillation, measured in plane perpendicular to hinge line, radians except as noted
$\phi$	amplitude of all-movable-control roll oscillation, radians except as noted
$\omega$	angular frequency of oscillation, radians/sec
$\left. \begin{matrix} C_{h_{\delta,\omega}}, & C_{L_{\alpha,\omega}}, \\ C_{m_{\alpha,\omega}}, & C_{l_{\phi,\omega}} \end{matrix} \right\}$	derivative with respect to $\delta$ , $\alpha$ , or $\phi$ as noted
$C_{h_{\dot{\delta},\omega}}$	derivative with respect to $\frac{\dot{\delta}c_t}{2V}$
$C_{L_{\dot{\alpha},\omega}}, \quad C_{m_{\dot{\alpha},\omega}}$	derivative with respect to $\frac{\dot{\alpha}c_r}{2V}$
$C_{l_{\dot{\phi},\omega}}$	derivative with respect to $\frac{\dot{\phi}c_r}{2V}$
Subscript:	
$\omega$	derivative obtained from an oscillation

## DISCUSSION OF RESULTS

## Flap-Type Controls

The aerodynamic hinge moment existing on the oscillating flap-type controls discussed herein is represented in complex notation by the relationship

$$\frac{\text{Resultant hinge moment}}{2M'q\delta} = C_{h\delta,\omega} + ik_{\delta}C_{h\dot{\delta},\omega}$$

where  $C_{h\delta,\omega}$  represents an aerodynamic spring-moment derivative proportional to the component of the total aerodynamic moment in phase with control position. The product  $k_{\delta}C_{h\dot{\delta},\omega}$  is an aerodynamic damping parameter, proportional to the component of the total aerodynamic moment in phase with control rotational velocity, and contributes the damping. The part  $C_{h\dot{\delta},\omega}$  represents an aerodynamic viscous-damping derivative.

Theoretical considerations.— Theoretical values for control aerodynamic damping are shown in figure 1. These two-dimensional-flow results were obtained from references 1 to 3 and are presented to provide a framework for evaluating the experimental flap-type-control data. Theoretical damping derivatives are plotted against Mach number for a 30-percent-chord flap-type control hinged at the leading edge. The dotted portion of the lines is an arbitrary fairing between the subsonic and supersonic theories, and the Mach number variation indicated is in general agreement with experiment. Theory shows the aerodynamic damping to be unstable for some values of reduced frequency at Mach numbers from about 0.9 to 1.5. In this region, control-surface flutter can occur unless sufficient nonaerodynamic damping is present in the control system to provide damping moments greater than the unstable aerodynamic moments. The subsonic and supersonic damping derivatives are fairly independent of Mach number and reduced frequency. However, large effects are indicated at transonic speeds, and the idealized theory indicates stable damping for reduced frequencies representing very high oscillating frequencies. Experimental damping results to date (refs. 4 to 11) have all been in the frequency range where theory indicates instability, and these experimental data show unstable damping in the control rotational mode at transonic speeds. The magnitudes indicated by test and theory are often in poor agreement, but this is not surprising considering the mixed-flow conditions which exist at transonic speeds and the possible influence from nonpotential sources. Based on these results, a fundamental approach in alleviating control-surface "buzz" would be to provide enough nonaerodynamic damping in the control system to overcome the unstable aerodynamic effects. This approach generally necessitates the addition of some type of artificial

damping to the control system, for example, the type provided by a hydraulic damper. This addition can often lead to mechanical complexities, especially when such factors as control free play are considered; and it would be desirable to stabilize the control aerodynamic damping by some change in geometric characteristics provided overall control efficiency can be maintained.

Control hinge position and profile shape are known to have large effects on static hinge moments, and some of their effects on dynamic hinge moments have recently been determined in the hope that stable control aerodynamic damping at transonic speeds can be achieved.

Effects of hinge position.- Studies of the effects of control hinge position and profile shape were made in the Langley high-speed 7- by 10-foot tunnel with the wing-control configuration shown in figure 2 (refs. 7 and 8). These tests were at a Reynolds number of about  $2 \times 10^6$  based on the wing mean aerodynamic chord. Model plan form was held constant and the total control chord was 30 percent of the wing chord. The range of test conditions covered is indicated in figure 2. From figure 1 it can be seen that the test frequencies are in a range where two-dimensional-flow theory indicates unstable aerodynamic damping at transonic speeds for a 30-percent-chord control hinged at the leading edge. This paper first presents the effects of hinge-line position, as indicated by results for the three conventional control profiles shown in figure 2, and then summarizes the effects of the profile modifications indicated. The hinge line is located by the ratio of the balance chord  $c_b$  to the chord of the control rearward of the hinge line  $c_a$ , and 20-, 35-, and 100-percent-overhang balanced controls were tested.

In figure 3 the effects of hinge position on the control aerodynamic damping are summarized. These data are presented for a reduced frequency of 0.10 and an angle of attack of  $0^\circ$ ; in general, the variations in angle of attack and reduced frequency covered in these tests had small effects on the control hinge-moment results. A free-oscillation test technique was used and the damping derivative is plotted against oscillation amplitude for representative test Mach numbers in figure 3(a) with the complete Mach number variation shown in figure 3(b) for low oscillation amplitudes. Positive values of  $C_{h\delta, \omega}$  indicate unstable aerodynamic damping. The flutter or buzz associated with the unstable damping shown for this model was a self-excited oscillation and built up in amplitude until the aerodynamic energy fed into the control system over a complete cycle was balanced by the energy dissipated due to structural and frictional damping. Steady-state flutter points for the test control system are indicated by the circular symbols in figure 3(a). The damping derivative for the 20- and 35-percent-overhang balanced controls at subsonic speed was stable and fairly constant to oscillation amplitudes of about  $10^\circ$ . Damping for the 100-percent-overhang balanced control was nonlinear with amplitude

at this speed and unstable at the higher oscillation amplitudes. In order to initiate the model flutter shown for this subsonic Mach number, it was necessary to displace initially the control to some intermediate amplitude and suddenly release it. This instability at a low Mach number is believed to be closely related to a stall-flutter type of phenomenon. Increasing the Mach number into the transonic speed range caused the control aerodynamic damping to become unstable for all hinge positions tested. For the 100-percent-overhang balanced control there was first a large stable increase in damping with increasing Mach number before the damping became unstable. Model flutter at these transonic speeds was initiated by random tunnel disturbances, and the flutter amplitude was markedly decreased at sonic speed with the hinge located at the control midchord. The damping at transonic speeds was nonlinear with amplitude for all hinge positions and indicated the influence of nonpotential effects which restrict the application of any potential theory.

Shown in figure 4 are recent control aerodynamic damping results obtained from a free-flight rocket-powered-model test by the Langley Pilotless Aircraft Research Division. These data were obtained by a free-oscillation test technique similar to that described in reference 10. Test Reynolds number, based on the wing mean aerodynamic chord, varied from  $2 \times 10^6$  to  $13 \times 10^6$ . The delta-wing configuration is illustrated and the trailing-edge flap-type control was hinged slightly rearward of the control midchord. The experimental damping derivative evaluated for an oscillation amplitude of  $1.8^\circ$  is shown for Mach numbers from about 0.5 to 1.9, and the test reduced frequency varied as indicated through the Mach number range. For this midchord hinge position, there was a large increase in stable damping at high subsonic speeds and unstable aerodynamic damping in the transonic Mach number region, with the damping again becoming stable at the higher test supersonic speeds. These aerodynamic damping trends with Mach number, measured in free flight, are in agreement with the theoretical and wind-tunnel results presented. Based on the data shown in figures 3 and 4, reasonable hinge positions do not offer much promise in alleviating the unstable damping in the control rotational mode at transonic speeds.

The effects of hinge position and Mach number on the control in phase or stiffness derivative for the wind-tunnel model are presented in figure 5. Derivatives obtained from dynamic and static tests are compared to illustrate the effects of oscillating the control. Positive values of this derivative indicate overbalanced or statically unstable hinge moments. The balancing effect of shifting the hinge line rearward is shown, and the midchord hinge position overbalances the control throughout the speed range tested. The oscillating spring moments are approximately equal to the static values for the 20- and 35-percent-overhang balanced controls, and the differences shown for the 100-percent-overhang

balanced control can be attributed to the larger deflection range over which it was necessary to evaluate the stiffness derivative for the dynamic tests. This agreement indicates that, for a wide range of hinge positions, static hinge moments can be used to predict accurately the frequency of control buzz.

Effects of profile shape.- The profile modifications studied in the wind-tunnel investigation are illustrated in figure 2. For the 20-percent-overhang balanced control the thickness at the trailing edge was made equal to the hinge-line thickness, and the portion of the control forward of the hinge was not altered. Results for the oscillating hinge moments for this control were similar to the results for the original profile with the aerodynamic damping still unstable at transonic speeds. This modification caused a slight beneficial shift in the level of unstable damping and an increase in the aerodynamic spring stiffness; however, the flutter characteristics of the model were not appreciably improved. (See ref. 7.)

On the 35-percent-overhang balanced control two profile changes were made. For the lower modification shown, the rear half of the conventional control chord was replaced by a thin "splitter" plate over essentially the full span of the control. This control was similar to some controls tested in a flight investigation by North American Aviation, Inc. (For example, see ref. 12.) In the present tunnel tests, the oscillating hinge-moment and flutter results measured for this splitter-plate control did not show any significant differences relative to the original profile, and the aerodynamic damping indicated about the same level of instability at Mach numbers from about 0.92 to 1.01, the maximum speed tested. In reference 12 a trailing-edge splitter plate combined with a slight thickening of the forward portion of the control has given qualitative indication of improved buzz stability. Direct comparison of the model and flight results is not feasible since the aerodynamic damping was not measured in flight, and there are appreciable geometric differences between the configurations.

The "wedge" modification to the 35-percent-overhang balanced control did give some beneficial effects on control damping. The trailing-edge thickness was a little more than twice the thickness tested on the modified 20-percent-overhang balanced control. The leading and trailing edges were connected by a straight line which resulted in an increase in the hinge-line thickness relative to the original profile. Damping results for the wedge control are shown in figure 6 and are compared with the damping of the conventional profile. The aerodynamic damping of the wedge control was stable at low oscillation amplitudes for the complete-test speed range. However, at transonic speeds, stability is confined to oscillation amplitudes less than about  $3^{\circ}$ . Damping for the wedge control is unstable for amplitudes greater than about  $3^{\circ}$ ; if the



model wedge control is manually displaced to these unstable amplitudes and released, it would flutter with characteristics very similar to those in the response of the conventional control.

### All-Movable Control

The model used to measure some oscillating aerodynamic derivatives at transonic speeds for conditions of particular application to all-movable controls is shown in figure 7. These tests were made in the Langley 2-foot transonic flutter tunnel at Reynolds numbers, based on the control mean aerodynamic chord, from  $1.4 \times 10^6$  to  $3.6 \times 10^6$ . The rigid-body degrees of freedom in pitch and roll to be considered are illustrated. The pitch axis passes through the midchord at the root and the leading edge at the tip. The roll axis was arbitrarily chosen inboard of the model root, and the pitch and roll motion together with the angles describing the modes are illustrated. Nomenclature similar to that used in discussing the flap-type controls is also used for this all-movable control with the resultant aerodynamic forces and moments reduced to derivatives that are either in or out of phase with the motion. The aerodynamic forces and moments existing on the oscillating model are represented in complex notation for pitching motion as

$$\frac{\text{Resultant lift}}{qS\alpha} = C_{L_{\alpha},\omega} + ik_{\alpha}C_{L_{\dot{\alpha}},\omega}$$

$$\frac{\text{Resultant pitching moment}}{qS \frac{c_r}{2} \alpha} = C_{m_{\alpha},\omega} + ik_{\alpha}C_{m_{\dot{\alpha}},\omega}$$

and for rolling motion as

$$\frac{\text{Resultant rolling moment}}{qS \frac{c_r}{2} \phi} = C_{l_{\phi},\omega} + ik_{\phi}C_{l_{\dot{\phi}},\omega}$$

Lift and pitching-moment derivatives are presented for the pitching motion, and the damping due to roll is shown for the rolling oscillation. These experimental data have not yet been compared with existing three-dimensional-flow theory (refs. 13 and 14).

Lift components due to pitch oscillation of the model are shown in figure 8, and these data were evaluated for a forced-oscillation amplitude of about  $3^\circ$  to each side of  $0^\circ$  angle of attack. The lift in phase with the motion is shown on the left and the out-of-phase component is shown on the right. Data were measured for a Mach number range from 0.6 to 1.2, and the curves represent values for various reduced frequencies.

For a constant reduced frequency, the in-phase derivative increases with Mach numbers from 0.6 to 1.0 and decreases with Mach numbers from 1.0 to 1.2. The out-of-phase derivative decreases with increasing Mach numbers from 0.6 to 1.0 and changes sign from positive to negative near a Mach number of 1.0. Increasing the reduced frequency decreases the in-phase component of the total lift at all test speeds and causes a positive increment in the magnitude of the out-of-phase component. Although it is not presented herein, experimental data have shown that the rolling moments due to pitch oscillation follow the same trends as those shown herein for the lift.

In figure 9 the pitch-damping parameter due to pitch oscillation of the control is plotted as a function of reduced frequency and Mach number. These aerodynamic data were evaluated from the free-oscillation response of the control following removal of the forcing function at an oscillation amplitude of about  $3^\circ$ . For additional information on the test technique used, see references 15 and 16. The aerodynamic viscous-damping derivative was essentially linear for amplitudes from  $0^\circ$  to  $3^\circ$ . The damping moments were stable throughout the complete Mach number range from 0.6 to 1.2, and there was a tendency for the damping parameter to become more stable up to  $M \approx 1.0$  and then decrease. The damping increased as the reduced frequency was increased. For conditions roughly approximating those of the present tests, two-dimensional-flow theory (refs. 2 and 3) indicates unstable values for this parameter at transonic speeds. However, three-dimensional-flow theory (refs. 13 and 14) indicates a rather large stabilizing effect at these speeds due to aspect ratio; therefore, these experimental results showing stable damping appear to be in reasonable agreement with existing theory.

Figure 10 shows the roll-damping parameter due to roll oscillation of the control as a function of reduced frequency and Mach number. These data were evaluated from the free-oscillation response of the control following roll oscillations up to amplitudes  $\phi$  of about  $3^\circ$ . The roll-damping moments were stable throughout the speed range tested, and the damping tends to become more stable as the test Mach number is increased. Increasing the reduced frequency also increases the stable damping-in-roll parameter.

#### CONCLUDING REMARKS

The aerodynamic forces and moments acting on oscillating flap-type and all-movable control surfaces at transonic speeds have been summarized. The discussion on flap-type controls has briefly reviewed what could be considered the fundamental approach in alleviating one-degree-of-freedom flutter of this type of control, namely, incorporating sufficient non-aerodynamic damping in the control system to overcome the unstable

~~CONFIDENTIAL~~

aerodynamic moments. Experimental results were presented which establish the general magnitude of the unstable aerodynamic moments for the test models. However, it is desirable to have a control configuration with inherent aerodynamic stability; therefore, the aerodynamic effects of control hinge-line position and some profile modifications were studied. Based on these results, no significant benefits in control aerodynamic damping were obtained for a wide range of hinge positions. Of three control profile modifications tested, only a "wedge" modification to a 35-percent-overhang balanced control gave significant improvements in "buzz" stability. This wedge control gave stable aerodynamic damping in the control rotational mode up to the maximum speed tested. However, the stable damping and improvement in flutter characteristics were limited to oscillation amplitudes less than about  $3^\circ$ .

For an all-movable control, the oscillating aerodynamic derivatives which define the separate effects of rigid-body pitch and rigid-body roll have been presented through the transonic speed range. The aerodynamic damping for this all-movable control was stable at all conditions tested.

Langley Aeronautical Laboratory,  
National Advisory Committee for Aeronautics,  
Langley Field, Va., March 7, 1957.

~~CONFIDENTIAL~~

## REFERENCES

1. Anon.: Tables of Aerodynamic Coefficients for an Oscillating Wing-Flap System in a Subsonic Compressible Flow. Rep. F.151, Nationaal Luchtvaartlaboratorium, Amsterdam, May 1954.
2. Nelson, Herbert C., and Berman, Julian H.: Calculations on the Forces and Moments for an Oscillating Wing-Aileron Combination in Two-Dimensional Potential Flow at Sonic Speed. NACA Rep. 1128, 1953. (Supersedes NACA TN 2590.)
3. Garrick, I. E., and Rubinow, S. I.: Flutter and Oscillating Air-Force Calculations for an Airfoil in a Two-Dimensional Supersonic Flow. NACA Rep. 846, 1946. (Supersedes NACA TN 1158.)
4. Reese, David E., Jr.: An Experimental Investigation at Subsonic and Supersonic Speeds of the Torsional Damping Characteristics of a Constant-Chord Control Surface of an Aspect Ratio 2 Triangular Wing. NACA RM A53D27, 1953.
5. Martin, Dennis J., Thompson, Robert F., and Martz, C. William: Exploratory Investigation of the Moments on Oscillating Control Surfaces at Transonic Speeds. NACA RM L55E31b, 1955.
6. Reese, David E., Jr., and Carlson, William C. A.: An Experimental Investigation of the Hinge-Moment Characteristics of a Constant-Chord Control Surface Oscillating at High Frequency. NACA RM A55J24, 1955.
7. Thompson, Robert F., and Moseley, William C., Jr.: Oscillating Hinge Moments and Flutter Characteristics of a Flap-Type Control Surface on a 4-Percent-Thick Unswept Wing With Low Aspect Ratio at Transonic Speeds. NACA RM L55K17, 1956.
8. Thompson, Robert F., and Moseley, William C., Jr.: Effect of Hinge-Line Position on the Oscillating Hinge Moments and Flutter Characteristics of a Flap-Type Control at Transonic Speeds. NACA RM L57C11, 1957.
9. Tuovila, W. J., and Hess, Robert W.: Aerodynamic Damping at Mach Numbers of 1.3 and 1.6 of a Control Surface on a Two-Dimensional Wing by the Free-Oscillation Method. NACA RM L56A26a, 1956.
10. Martz, C. William: Experimental Hinge Moments on Freely Oscillating Flap-Type Control Surfaces. NACA RM L56G20, 1956.

11. Clevenson, Sherman A.: Some Wind-Tunnel Experiments on Single-Degree-of-Freedom Flutter of Ailerons in the High Subsonic Speed Range. NACA TN 3687, 1956. (Supersedes NACA RM L9B08.)
12. Anon.: Flight Test Progress Report No. 23 for Period Ending 7 October 1955 for Model FJ-4 Airplanes. Rep. No. NA 54H-374-23 (Contract NOa(s)54-323), North American Aviation, Inc., Oct. 20, 1955.
13. Nelson, Herbert C., Rainey, Ruby A., and Watkins, Charles E.: Lift and Moment Coefficients Expanded to the Seventh Power of Frequency for Oscillating Rectangular Wings in Supersonic Flow and Applied to a Specific Flutter Problem. NACA TN 3076, 1954.
14. Runyan, Harry L., and Woolston, Donald S.: Method for Calculating the Aerodynamic Loading on an Oscillating Finite Wing in Subsonic and Sonic Flow. NACA TN 3694, 1956.
15. Clevenson, Sherman A., and Widmayer, Edward, Jr.: Experimental Measurements of Forces and Moments on a Two-Dimensional Oscillating Wing At Subsonic Speeds. NACA TN 3686, 1956. (Supersedes NACA RM L9K28a.)
16. Widmayer, Edward, Jr., Clevenson, Sherman A., and Leadbetter, Sumner A.: Some Measurements of Aerodynamic Forces and Moments at Subsonic Speeds on a Rectangular Wing of Aspect Ratio 2 Oscillating About the Midchord. NACA RM L53F19, 1953.

# THEORETICAL CONTROL DAMPING TWO-DIMENSIONAL THEORY

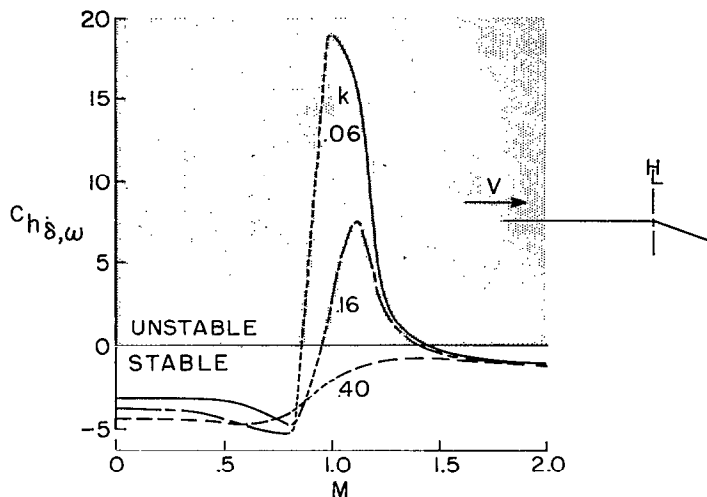


Figure 1

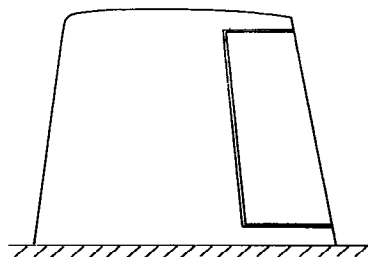
## FLAP-TYPE CONTROL MODEL WIND-TUNNEL TESTS

### MODEL PARAMETERS

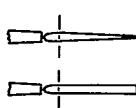
ASPECT RATIO 1.8  
TAPER RATIO 0.74  
NACA 64A004

### SCOPE OF TESTS

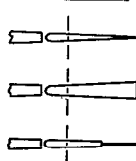
M 0.6 TO 1.01  
ANGLE OF ATTACK 0° AND 6°  
REDUCED FREQUENCY 0.06 TO 0.13



$$c_b = 0.20 c_a$$



$$c_b = 0.35 c_a$$



$$c_b = c_a$$

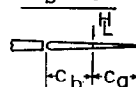


Figure 2

## EFFECT OF HINGE POSITION ON CONTROL DAMPING

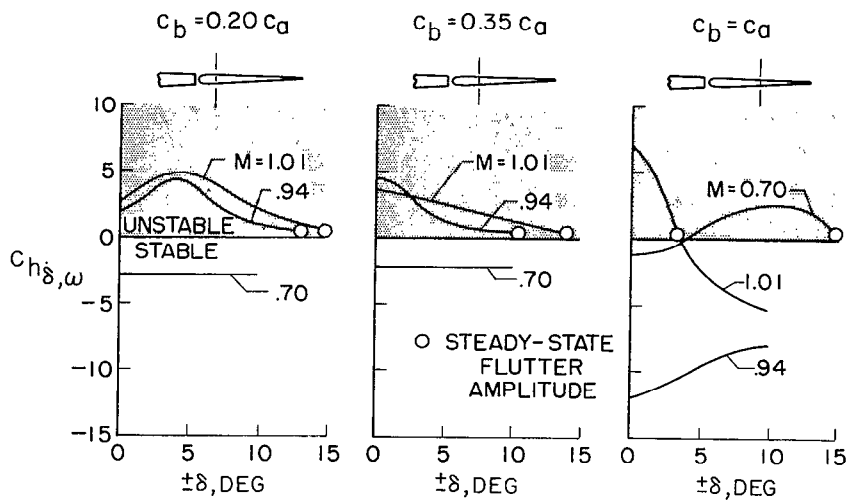
 $k=0.10$ ;  $\alpha=0^\circ$ 

Figure 3(a)

## EFFECT OF HINGE POSITION ON CONTROL DAMPING

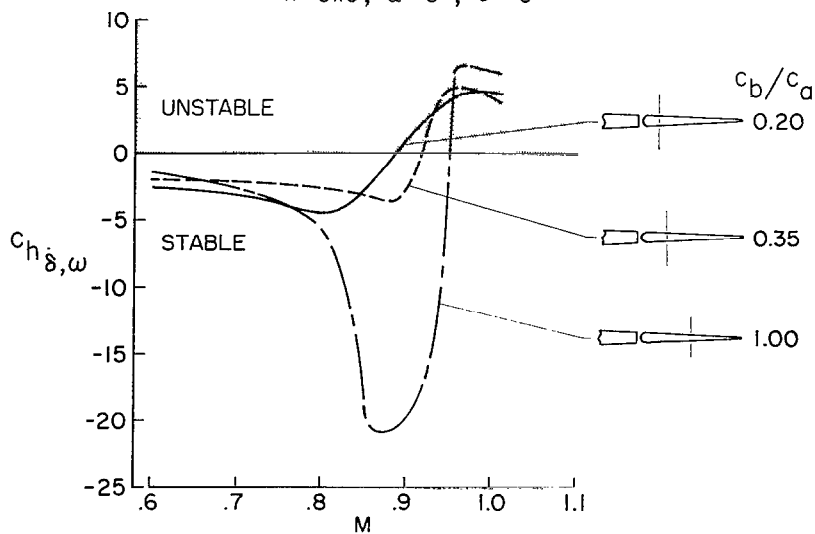
 $k=0.10$ ;  $\alpha=0^\circ$ ;  $\delta \approx 0^\circ$ 

Figure 3(b)

EFFECT OF MACH NUMBER ON CONTROL DAMPING  
ROCKET-MODEL TEST;  $\delta = \pm 1.8^\circ$ ;  $\alpha = 0^\circ$

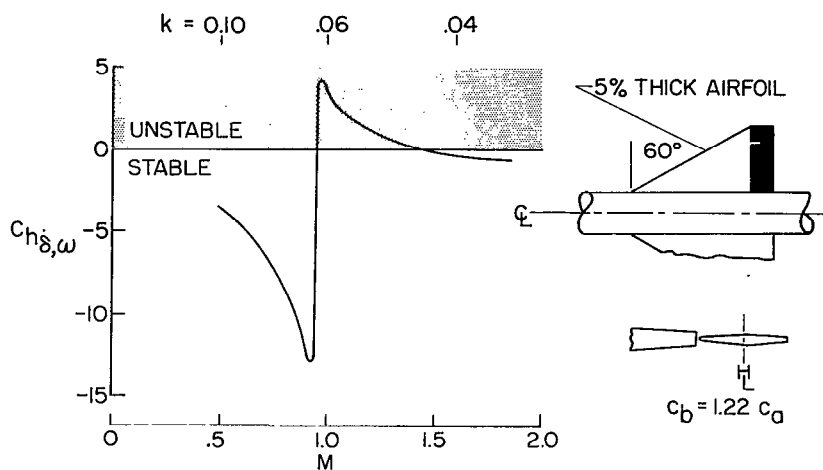


Figure 4

EFFECT OF HINGE POSITION ON CONTROL STIFFNESS

$k = 0.10, \alpha = 0^\circ$

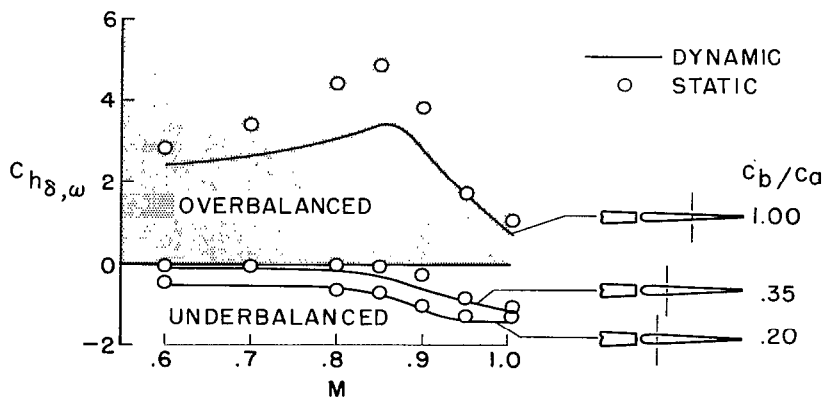


Figure 5



## EFFECT OF WEDGE PROFILE ON CONTROL DAMPING

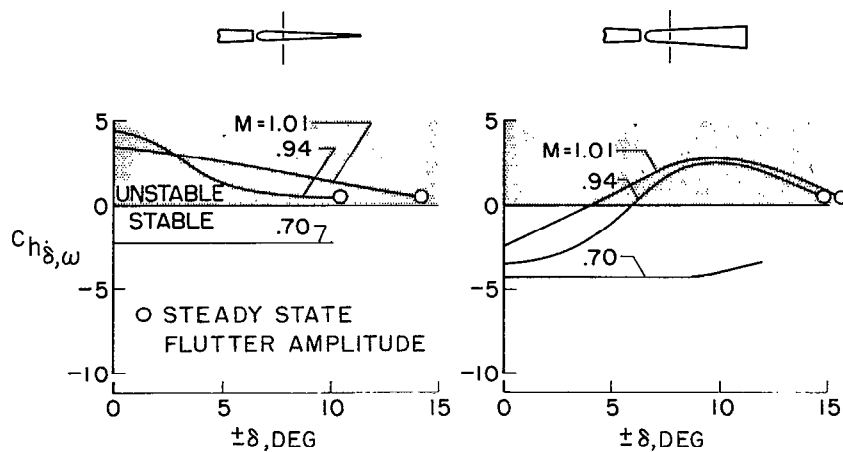
 $k=0.10 ; \alpha=0^\circ$ 

Figure 6

## ALL-MOVABLE CONTROL SURFACE

RIGID-BODY DEGREES OF FREEDOM

PANEL ASPECT RATIO = 1.25

TAPER RATIO = 0.283

NACA 65A005

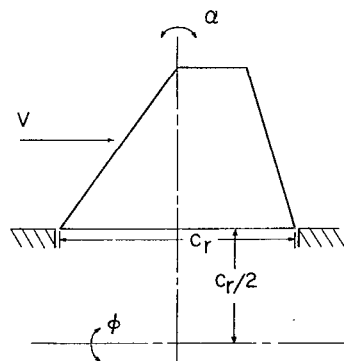


Figure 7

## EFFECT OF MACH NUMBER ON LIFT COMPONENTS DUE TO PITCH OSCILLATION

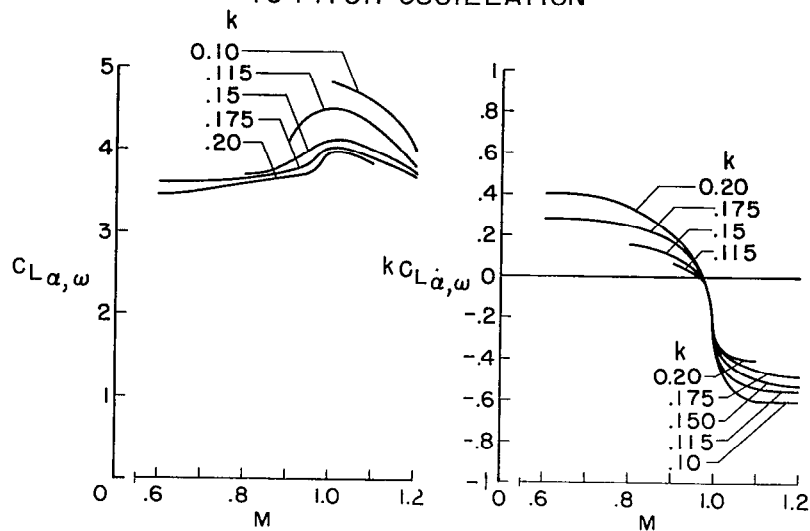


Figure 8

## EFFECT OF MACH NUMBER ON PITCH-DAMPING COMPONENT DUE TO PITCH OSCILLATION

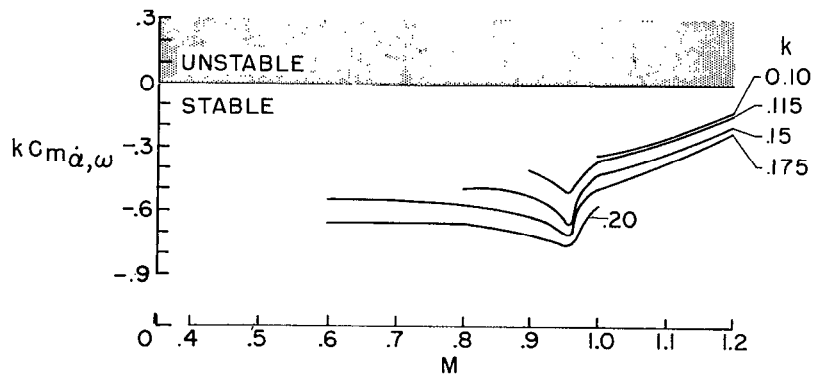


Figure 9

EFFECT OF MACH NUMBER ON ROLL-DAMPING  
COMPONENT DUE TO ROLL OSCILLATION

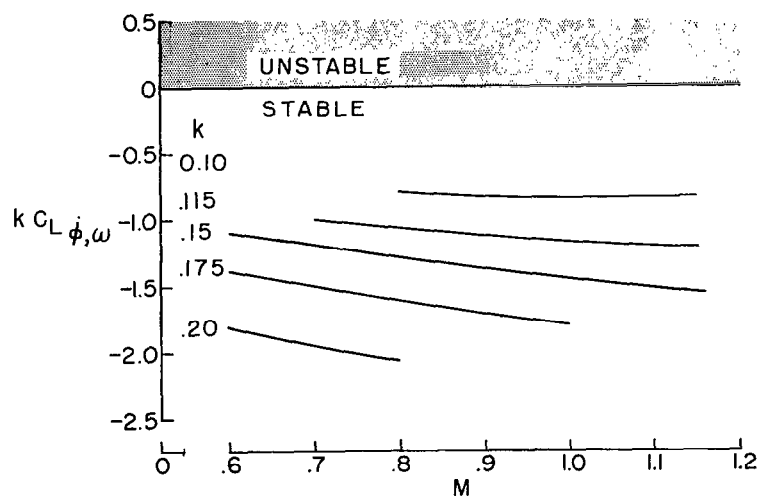
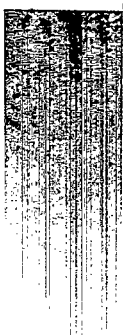


Figure 10

NASA Technical Library



3 1176 01437 9151



CONFIDENTIAL